Fault diagnosis of a Wind Turbine Rotor using a Multi-blade Coordinate Framework

Henriksen, Lars Christian; Niemann, Hans Henrik; Poulsen, Niels Kjølstad

Published in:
Fault Detection, Supervision and Safety of Technical Processes

Link to article, DOI:
10.3182/20120829-3-MX-2028.00258

Publication date:
2012

Document Version
Publisher's PDF, also known as Version of record

Preprints of the 8th IFAC Symposium on Fault Detection,
Supervision and Safety of Technical Processes (SAFEPROCESS)
August 29-31, 2012. Mexico City, Mexico

Fault diagnosis of a Wind Turbine Rotor using a Multi-blade Coordinate Framework ⋆

Lars Christian Henriksen * **Hans Henrik Niemann** **
Niels Kjølstad Poulsen ***

* *Dept. of Wind Energy, Technical University of Denmark, (e-mail: larh@dtu.dk)*
** *Dept. of Electrical Engineering, Technical University of Denmark, (e-mail: hhn@elektro.dtu.dk)*
*** *Dept. of Informatics and Mathematical Modelling, Technical University of Denmark, (e-mail: nkp@imm.dtu.dk)*

Abstract:
Fault diagnosis of a wind turbine rotor is considered. The faults considered are sensor faults and blades mounted with a pitch offset. A fault at a single blade will result in asymmetries in the rotor, which can be applied for fault diagnosis. The diagnosis is derived by using the multi-blade coordinate (MBC) transformation also known as the Coleman transformation together with active fault diagnosis (AFD). This transforms the setup from rotating to fixed frame coordinates. The rotor speed acts as the auxiliary input for the active diagnosis. The applied method take the varying rotor speed into account. Operation at different mean wind speeds is examined and it is discussed how to exploit the findings acquired by the investigation of the various faults.

Keywords: Wind Turbine, Fault Diagnosis

1. INTRODUCTION

In order to improve operation of wind turbines with respect to economy, condition monitoring, fault diagnosis and fault tolerant control are important tools that can be used to detect faults and determine the prober action.

The wind turbine can be subjected to various faults on various components: Using continuous wavelet transformation (CWT) Tsai et al. [2006] looked at blade damage detection and Watson et al. [2010] have investigated generator and drive train faults with CWT analysis of the generator power output sensor. Rotor condition monitoring for a number of different blade-specific faults have been examined by Caselitz and Giebhardt [2005].

Observer-based techniques for residual generation fault detection Frank and Ding [1994] on the other hand, take both the sensors and control actions into account and are thus able to detect faults even in closed-loop operation. To further enhance the fault diagnosis, active measures can be taken. In e.g. Niemann [2006], Poulsen and Niemann [2009] an auxiliary signal is injected into the system to aid the fault diagnosis.

Observer-based fault detection techniques have previously been applied on wind turbines e.g. Odgaard et al. [2009], Odgaard and Stoustrup [2010] and Wei and Verhaegen [2011]. For an overview of various fault detection and condition monitoring algorithms applied to wind turbines Hameed et al. [2009] can be consulted.

The multi-blade coordinate (MBC) transformation also denoted the Coleman transformation Coleman and Feingold [1958] enables a time-varying system to be transformed to a time-invariant system, when the rotor of the wind turbine, helicopter etc. is assumed isotropic, i.e. symmetric. MBC for dynamical analysis of the wind turbine is a strong tool and e.g. Hansen [2003] and Bir [2008] discusses the subject in much greater depth. If asymmetries do occur, the MBC transformed system will not be time-invariant. This property can be exploited to ease the fault diagnosis. The transformation of the wind turbine model, the nominal case will have zero-mean residuals and the faulty case will have non-zero-mean residuals. Furthermore, the strength of MBC is that time-varying system becomes time-invariant and that a individual pitching controller is easily described.

In this paper a wind turbine subjected to fault diagnosis is presented. The considered faults are offset in pitch actuator, offset on edgewise and flapwise strain gauge sensors for each blade. An observer-based residual generator will be applied and the residuals will be analyzed by a CUSUM test to detect and isolate faults. The rotation of the wind turbine acts as a natural injection of a periodic signal, which can be detected in the residuals in the faulty case. The varying rotor speed result in an injected signal with varying frequency. The presented detection method is able to handle the varying rotor speed and results show good

⋆ This work was supported in part by the CASED Project funded by grant DSF-09-063197 of the Danish Council for Strategic Research.

detection performance even in the presence of varying rotor speed.

Simulations are performed in the multi-body aero-servo-elastic software HAWC2 Larsen and Hansen [2007] developed by Risø DTU. The wind turbine used in the simulations is the 5 MW reference wind turbine defined in Jonkman et al. [2009]. The applied nominal model does not include all the degrees of freedom included in the HAWC2 simulation model. Accordingly, the nominal case is not entirely nominal and residuals are expected to have mean values different from zero even in the nominal case. The task is then to determine the nominal conditions and detect if the residuals differ from the nominal values.

A preliminary investigation of fault detection of the wind turbine rotor is given in Henriksen et al. [2011].

The outline of this paper is as follows: The MBC transformation and its application to state space models is explained in Section 2 together with a presentation of the wind turbine model. The AFD approach is described in Section 3 including a discussion of the implementation by using an Extended Kalman filter. Simulation results are shown in Section 4. Finally, conclusions are drawn in Section 5.

2. MODEL FORMULATION

2.1 Multi-blade Coordinate Transformation

The Multi-blade Coordinate (MBC) Transformation enables the transformation from a rotating frame of reference to a fixed frame of reference. The azimuth angle ϕ_i of each blades $i = 1, \ldots, n_b$, assuming constant rotor speed Ω and equal angular spacing between the blades, is given by

$$\phi_i = \phi_0 + \Omega t - (i-1)\pi/n_b \qquad i = 1, \ ... \ n_b \tag{1}$$

and renders the MBC transformation a function of time t rather than the azimuth angle ϕ_i. For a 3-blades rotor, the azimuth angles can be combined in a vector, which is $\boldsymbol{\phi} = [\phi_1 \ \phi_2 \ \phi_3]^T$. The temporal argument of states and transformation matrices in the following has been omitted to simplify notation. The rotating frame coordinates $\boldsymbol{q}$ and the fixed frame coordinates $\boldsymbol{q^f}$ have the following relationship

$$\boldsymbol{q^f} = \mathbf{M}\boldsymbol{q} \qquad \boldsymbol{q} = \mathbf{M}^{-1}\boldsymbol{q^f}$$

where the MBC transformation matrices are

$$\mathbf{M} = \begin{bmatrix} \frac{1}{3}\mathbf{1}^T \\ \frac{2}{3}\cos\boldsymbol{\phi}^T \\ \frac{2}{3}\sin\boldsymbol{\phi}^T \end{bmatrix}, \quad \mathbf{M}^{-1} = \begin{bmatrix} \mathbf{1}^T \\ \cos\boldsymbol{\phi}^T \\ \sin\boldsymbol{\phi}^T \end{bmatrix}^T,$$

and $\mathbf{1} = [1 \ 1 \ 1]^T$, $\cos\boldsymbol{\phi} = [\cos\phi_1 \ \cos\phi_2 \ \cos\phi_3]^T$ and similarly for $sin(\phi)$.

$$\boldsymbol{q} = \mathbf{M}^{-1}\boldsymbol{q^f} \tag{2a}$$
$$\dot{\boldsymbol{q}} = \dot{\mathbf{M}}^{-1}\boldsymbol{q^f} + \mathbf{M}^{-1}\dot{\boldsymbol{q}}^{\boldsymbol{f}} \tag{2b}$$
$$\ddot{\boldsymbol{q}} = \ddot{\mathbf{M}}^{-1}\boldsymbol{q^f} + 2\dot{\mathbf{M}}^{-1}\dot{\boldsymbol{q}}^{\boldsymbol{f}} + \mathbf{M}^{-1}\ddot{\boldsymbol{q}}^{\boldsymbol{f}} \tag{2c}$$

where (2a) is the base transformation and (2b) is derived from $\dot{\boldsymbol{q}} = \frac{d}{dt}(\mathbf{M}^{-1}\boldsymbol{q^f})$ and 2c from $\ddot{\boldsymbol{q}} = \frac{d}{dt}(\dot{\mathbf{M}}^{-1}\boldsymbol{q^f} + \mathbf{M}^{-1}\dot{\boldsymbol{q}}^{\boldsymbol{f}})$. Here:

$$\dot{\mathbf{M}}^{-1} = \Omega \begin{bmatrix} \mathbf{0}^T \\ -\sin\boldsymbol{\phi}^T \\ \cos\boldsymbol{\phi}^T \end{bmatrix}^T \text{ and } \ddot{\mathbf{M}}^{-1} = \Omega^2 \begin{bmatrix} \mathbf{0}^T \\ -\cos\boldsymbol{\phi}^T \\ -\sin\boldsymbol{\phi}^T \end{bmatrix}^T$$

The inverse transformations are given by

$$\boldsymbol{q^f} = \mathbf{M}\boldsymbol{q} \tag{3a}$$
$$\dot{\boldsymbol{q}}^{\boldsymbol{f}} = \tfrac{2}{3}\dot{\mathbf{M}}^{-T}\boldsymbol{q} + \mathbf{M}\dot{\boldsymbol{q}} \tag{3b}$$
$$\ddot{\boldsymbol{q}}^{\boldsymbol{f}} = \tfrac{2}{3}\ddot{\mathbf{M}}^{-T}\boldsymbol{q} + \tfrac{4}{3}\dot{\mathbf{M}}^{-T}\dot{\boldsymbol{q}} + \mathbf{M}\ddot{\boldsymbol{q}} \tag{3c}$$

2.2 The MBC transformation applied on a state space model

A dynamic system in state space form can be expressed by a nonlinear ordinary differential equation vector function and a vector output function as

$$\dot{\boldsymbol{x}}(t) = \boldsymbol{f}(\boldsymbol{x}(t), \boldsymbol{u}(t), t) \tag{4a}$$
$$\boldsymbol{y}(t) = \boldsymbol{g}(\boldsymbol{x}(t), \boldsymbol{u}(t), t) \tag{4b}$$

where states $\boldsymbol{x}$, inputs $\boldsymbol{u}$, outputs $\boldsymbol{y}$ and the vector functions $\boldsymbol{f}$ and $\boldsymbol{g}$ are all functions of time. In the following, the temporal arguments of states, inputs and outputs and vector functions have been omitted to simplify notation.

First order Taylor expansion around the linearization $(\bar{\boldsymbol{x}}, \bar{\boldsymbol{u}})$ yields

$$\dot{\boldsymbol{x}} = \boldsymbol{f}(\bar{\boldsymbol{x}}, \bar{\boldsymbol{u}}) + \mathbf{A}(\boldsymbol{x} - \bar{\boldsymbol{x}}) + \mathbf{B}(\boldsymbol{u} - \bar{\boldsymbol{u}}) \tag{5a}$$
$$\boldsymbol{y} = \boldsymbol{g}(\bar{\boldsymbol{x}}, \bar{\boldsymbol{u}}) + \mathbf{C}(\boldsymbol{x} - \bar{\boldsymbol{x}}) + \mathbf{D}(\boldsymbol{u} - \bar{\boldsymbol{u}}) \tag{5b}$$

where the system matrices $(\mathbf{A}, \mathbf{B}, \mathbf{C}, \mathbf{D})$ are functions of time. The linearization can be rewritten to

$$\dot{\boldsymbol{x}} = \mathbf{A}\boldsymbol{x} + \mathbf{B}\boldsymbol{u} + \boldsymbol{\delta}, \quad \boldsymbol{\delta} = \boldsymbol{f}(\bar{\boldsymbol{x}}, \bar{\boldsymbol{u}}) - \mathbf{A}\bar{\boldsymbol{x}} - \mathbf{B}\bar{\boldsymbol{u}} \tag{6a}$$
$$\boldsymbol{y} = \mathbf{C}\boldsymbol{x} + \mathbf{D}\boldsymbol{u} + \boldsymbol{\gamma}, \quad \boldsymbol{\gamma} = \boldsymbol{g}(\bar{\boldsymbol{x}}, \bar{\boldsymbol{u}}) - \mathbf{C}\bar{\boldsymbol{x}} - \mathbf{D}\bar{\boldsymbol{u}} \tag{6b}$$

for typical linear control theory the pair $(\bar{\boldsymbol{x}}, \bar{\boldsymbol{u}})$ is chosen to be an equilibrium point (such that $\mathbf{0} = \boldsymbol{f}(\bar{\boldsymbol{x}}, \bar{\boldsymbol{u}})$), but the theory is also valid for other choices of $(\bar{\boldsymbol{x}}, \bar{\boldsymbol{u}})$.

A state space system description of a wind turbine with fixed frame degrees of freedom $\boldsymbol{x_1}$ e.g. tower fore-aft, rotor speed etc and rotating frame degrees of freedom $\boldsymbol{x_2} = [\boldsymbol{q} \ \dot{\boldsymbol{q}}]$ such as blade pitch angle $\boldsymbol{q}$ and blade pitch rate $\dot{\boldsymbol{q}}$. Fixed frame inputs $\boldsymbol{u_1}$ such as generator torque and rotating frame inputs $\boldsymbol{u_2}$ such as pitch angle reference

$$\boldsymbol{x} = \begin{bmatrix} \boldsymbol{x_1} \\ \boldsymbol{q} \\ \dot{\boldsymbol{q}} \end{bmatrix} \quad \boldsymbol{u} = \begin{bmatrix} \boldsymbol{u_1} \\ \boldsymbol{u_2} \end{bmatrix} \quad \boldsymbol{y} = \begin{bmatrix} \boldsymbol{x_1} \\ \dot{\boldsymbol{x}}_1 \\ \boldsymbol{q} \\ \dot{\boldsymbol{q}} \\ \ddot{\boldsymbol{q}} \end{bmatrix} \tag{7}$$

and outputs containing both rotating and fixed frame quantities.

The time-varying combined fixed and rotating frame system (7) can be transformed to a fixed frame time-invariant system where the states, inputs and outputs are transformed to the fixed frame of reference

$$\boldsymbol{x^f} = \mathbf{M_x}\boldsymbol{x} \text{ and } \boldsymbol{u^f} = \mathbf{M_u}\boldsymbol{u} \text{ and } \boldsymbol{y^f} = \mathbf{M_y}\boldsymbol{y}. \tag{8}$$

The MBC transformations gives the fixed frame system equations

$$\dot{\boldsymbol{x}}^{\boldsymbol{f}} = \mathbf{A^f}\boldsymbol{x^f} + \mathbf{B^f}\boldsymbol{u^f} + \delta^{\mathbf{f}} \tag{9a}$$
$$\boldsymbol{y^f} = \mathbf{C^f}\boldsymbol{x^f} + \mathbf{D^f}\boldsymbol{u^f} + \boldsymbol{\gamma^f} \tag{9b}$$

where

$$\mathbf{A^f} = \tilde{\mathbf{M}}_\mathbf{x}(\mathbf{A}\mathbf{M}_\mathbf{x}^{-1} - \dot{\mathbf{M}}_\mathbf{x}^{-1}), \qquad \mathbf{C^f} = \mathbf{M_y}\mathbf{C}\mathbf{M}_\mathbf{x}^{-1},$$
$$\mathbf{B^f} = \tilde{\mathbf{M}}_\mathbf{x}\mathbf{B}\mathbf{M}_\mathbf{u}^{-1}, \qquad \mathbf{D^f} = \mathbf{M_y}\mathbf{D}\mathbf{M}_\mathbf{u}^{-1},$$
$$\boldsymbol{\delta^f} = \tilde{\mathbf{M}}_\mathbf{x}\boldsymbol{\delta}, \qquad \boldsymbol{\gamma^f} = \mathbf{M_y}\boldsymbol{\gamma}.$$

The system matrices $(\mathbf{A^f}, \mathbf{B^f}, \mathbf{C^f}, \mathbf{D^f})$ are time-invariant, as are the residual vectors $(\boldsymbol{\delta^f}, \boldsymbol{\gamma^f})$ when rotating frame variables have been averaged in the linearization point

$$\bar{\boldsymbol{q}} = \text{mean}(\boldsymbol{q}) \text{ and } \bar{\dot{\boldsymbol{q}}} = \text{mean}(\dot{\boldsymbol{q}}).$$

The state equation MBC transformation matrices are

$$\tilde{\mathbf{M}}_\mathbf{x} = \begin{bmatrix} \mathbf{I} & & \\ & \mathbf{M} & \\ & & \mathbf{M} \end{bmatrix}, \quad \mathbf{M}_\mathbf{x}^{-1} = \begin{bmatrix} \mathbf{I} & & \\ & \mathbf{M}^{-1} & \\ & \dot{\mathbf{M}}^{-1} & \mathbf{M}^{-1} \end{bmatrix}$$

and

$$\dot{\mathbf{M}}_\mathbf{x}^{-1} = \begin{bmatrix} \mathbf{0} & & \\ & \dot{\mathbf{M}}^{-1} & \\ & \ddot{\mathbf{M}}^{-1} & 2\dot{\mathbf{M}}^{-1} \end{bmatrix}$$

For control signals and outputs the matrices are

$$\mathbf{M_u} = \begin{bmatrix} \mathbf{I} & \\ & \mathbf{M} \end{bmatrix} \text{ and } \mathbf{M_y} = \begin{bmatrix} \mathbf{I} & & & \\ & \mathbf{I} & & \\ & & \mathbf{M} & \\ & & & \mathbf{M} \end{bmatrix}$$

The nonlinear time discrete state progress equation

$$\boldsymbol{x}_{k+1}^{\boldsymbol{f}} = \underline{\boldsymbol{f}}^{\boldsymbol{f}}(\boldsymbol{x}_k^{\boldsymbol{f}}, \boldsymbol{u}_k^{\boldsymbol{f}}) = \boldsymbol{x}_k^{\boldsymbol{f}} + \int_{t_k}^{t_{k+1}} \dot{\boldsymbol{x}}^{\boldsymbol{f}}(\tau) d\tau \tag{10}$$

can be approximated by a linear description

$$\boldsymbol{x}_{k+1}^{\boldsymbol{f}} = \underline{\mathbf{A}}^{\mathbf{f}}\boldsymbol{x}_k^{\boldsymbol{f}} + \underline{\mathbf{B}}^{\mathbf{f}}\boldsymbol{u}_k^{\boldsymbol{f}} + \underline{\boldsymbol{\delta}}^{\boldsymbol{f}},$$
$$\underline{\boldsymbol{\delta}}^{\boldsymbol{f}} = \underline{\boldsymbol{f}}^{\boldsymbol{f}}(\bar{\boldsymbol{x}}^{\boldsymbol{f}}, \bar{\boldsymbol{u}}^{\boldsymbol{f}}) - \underline{\mathbf{A}}^{\mathbf{f}}\bar{\boldsymbol{x}}^{\boldsymbol{f}} - \underline{\mathbf{B}}^{\mathbf{f}}\bar{\boldsymbol{u}}^{\boldsymbol{f}} \tag{11}$$

and Henriksen and Poulsen [2010] gives further details regarding implementation.

2.3 MBC asymmetries

The MBC transformation for an isotropic rotor results in time-invariant quantities. In Henriksen et al. [2011] it was shown that additive and multiplicative perturbations result in different time-varying properties of the fixed frame coordinates: Additive perturbations give constant $\boldsymbol{q}_0$ and 1p-variation in $\boldsymbol{q}_c$ and $\boldsymbol{q}_s$. A multiplicative perturbation gives a 1p-variation of $\boldsymbol{q}_0$ and a 2p-variation in $\boldsymbol{q}_c$ and $\boldsymbol{q}_s$. These properties are exploited to detect for asymmetries in the rotor in the next sections.

2.4 Wind Turbine Model

The governing equations constituting the control design model used in Section 2.2 are presented in this section. The parameters of the control design model have been estimated system identification techniques Ljung [1999] on data from HAWC2 simulations. HAWC2 is a high fidelity simulation platform developed at Risø DTU.

The ordinary differential equations of the sub-models, are gathered in a state space ordinary differential equation and an output function in the form of (4) where $\boldsymbol{x}$ is the state vector, $\boldsymbol{u}$ is the input vector and $\boldsymbol{y}$ is the measurement vector. The vectors are comprised by the following variables

$$\boldsymbol{x} = [\Omega\ \Omega_g\ \Psi_\Delta\ \dot{\Psi}_\Delta\ V_{t,i}\ \dot{V}_{t,i}\ \bar{v}_{n,i}\ \theta_i\ \dot{\theta}_i\ Q_g]^T$$
$$\boldsymbol{u} = [\theta_{ref,i}\ Q_{g,ref}]^T$$
$$\boldsymbol{y} = [\Omega^m\ \Omega_g^m\ \ddot{\Psi}_t^m\ Q_{n,i}^{SG}\ Q_{t,i}^{SG}\ \theta_i^m\ \dot{\theta}_i^m\ \ddot{\theta}_i^m\ Q_g^m\ P_e^m]^T$$

Here the state variables are: angular velocity of the rotor (Ω), angular velocity of the generator (Ω_g), the deflection and its derivative of the tower (Ψ_Δ, $\dot{\Psi}_\Delta$), the wind speed and its derivative ($V_{t,i}$ and $\dot{V}_{t,i}$), the induction wind speed ($\bar{v}_{n,i}$), the ($n_b = 3$) blade pitches and their derivatives (θ_i and $\dot{\theta}_i$) and the generator torque (Q_g).

In the design model, the turbulent wind speed variation is modeled as a second order model. That is why the wind speed and its derivative ($V_{t,i}$ and $\dot{V}_{t,i}$) are in the state vector.

The control actions are the reference to the three pitch actuators and the reference to the generator (developing a specific torque on the drive train). The pitch actuators are modeled as second order systems while the generator is modeled as a first order system.

In the design model we assume to measure the angular rotor speed (Ω^m), the angular speed of the generator (Ω_g^m), the acceleration of the tower top position ($\ddot{\Psi}_t^m$), the generator torque (Q_g^m) and the produced electric power (P_e^m). For each blade we are measuring the root bending moments in edge and flap wise directions ($Q_{n,i}^{SG}$ and $Q_{t,i}^{SG}$), the actual pitch angles, their derivatives and their accelerations (θ_i^m, $\dot{\theta}_i^m$ and $\ddot{\theta}_i^m$).

A more detailed description of the wind turbine model, used by the proposed method, is omitted here, but the reader is referred to e.g. Henriksen et al. [2011] for further details.

3. FAULT DIAGNOSIS

In the following section, the theory for an active/passive fault diagnosis (FD) method is presented. The method is based on the passive fault diagnosis found in e.g. Frank and Ding [1994] and on the active fault diagnosis found in e.g. Niemann [2006], Niemann and Poulsen [2008].

The system shown in Fig. 1(a), is described by:

$$\boldsymbol{\Sigma_P} : \begin{cases} \boldsymbol{e} = \mathbf{G_{ed}}(\boldsymbol{p})\boldsymbol{d} + \mathbf{G_{eu}}(\boldsymbol{p})\boldsymbol{u} \\ \boldsymbol{y} = \mathbf{G_{yd}}(\boldsymbol{p})\boldsymbol{d} + \mathbf{G_{yu}}(\boldsymbol{p})\boldsymbol{u} \end{cases} \tag{12}$$

where the output vectors $\boldsymbol{e}$ and $\boldsymbol{y}$ are control objectives and measurements, respectively. The input vectors $\boldsymbol{d}$ and $\boldsymbol{u}$ are input disturbance and control vector, respectively. The transfer functions are functions of the parameter vector $\boldsymbol{p} = [p_1, \ldots]^T$, where $\boldsymbol{p} = \mathbf{0}$ is the nominal case. Further, let the system be controlled by a stabilizing controller

$$\boldsymbol{\Sigma_C} : \{\boldsymbol{u} = \mathbf{K}\boldsymbol{y} \tag{13}$$

The nominal system given by $\mathbf{G_{yu}}(\mathbf{0})$ and the stabilizing controller $\mathbf{K}$ can be subjected to a co-prime factorization

$$\mathbf{G_{yu}}(\mathbf{0}) = \mathbf{N}\mathbf{M}^{-1} = \tilde{\mathbf{M}}^{-1}\tilde{\mathbf{N}}, \ \mathbf{K} = \mathbf{U}\mathbf{V}^{-1} = \tilde{\mathbf{V}}^{-1}\tilde{\mathbf{U}} \tag{14}$$

where $\mathbf{N}$, $\mathbf{M}$, $\tilde{\mathbf{N}}$, $\tilde{\mathbf{M}}$, $\mathbf{U}$, $\mathbf{V}$, $\tilde{\mathbf{U}}$ and $\tilde{\mathbf{V}} \in \mathcal{RH}_\infty$ must satisfy the double Bezout equation Tay et al. [1997].

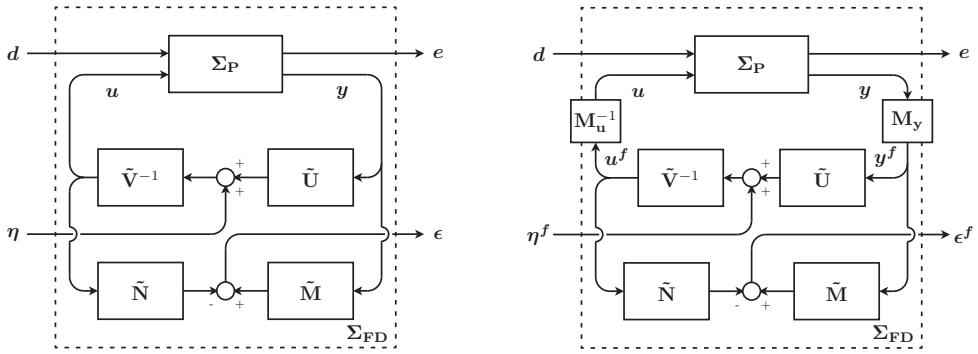

(a) FD setup in rotating frame coordinates

(b) FD setup in fixed frame coordinates

Fig. 1. Fault diagnosis setup.

3.1 Active fault diagnosis setup

Based on the coprime factorization in (14) a residual $\boldsymbol{\epsilon}$ for $\boldsymbol{\Sigma_P}$ is given by Niemann [2006]:

$$\boldsymbol{\epsilon} = \tilde{\mathbf{M}}\boldsymbol{y} - \tilde{\mathbf{N}}\boldsymbol{u} \tag{15}$$

This is the same residual generator used with passive fault diagnosis Frank and Ding [1994]. The fault diagnosis system setup, also seen in Fig. 1(a), is given by

$$\boldsymbol{\Sigma_{FD}} : \begin{cases} \boldsymbol{e} = \mathbf{P}_{\mathbf{ed}}(\boldsymbol{p})\boldsymbol{d} + \mathbf{P}_{e\eta}(\boldsymbol{p})\boldsymbol{\eta} \\ \boldsymbol{\epsilon} = \mathbf{P}_{\epsilon\mathbf{d}}(\boldsymbol{p})\boldsymbol{d} + \mathbf{P}_{\epsilon\eta}(\boldsymbol{p})\boldsymbol{\eta} \end{cases} \tag{16}$$

where $\boldsymbol{\eta}$ is an auxiliary input applied for active fault diagnosis. In the nominal case, the transfer function from $\boldsymbol{\eta}$ to $\boldsymbol{\epsilon}$ is zero and a zero-mean disturbance signal $\boldsymbol{d}$ will result in a zero-mean residual signal $\boldsymbol{\epsilon}$. This can be exploited to determine whether or not the observed system is in its nominal state or if $\boldsymbol{p} \neq \mathbf{0}$.

Instead of injecting an auxiliary input $\boldsymbol{\eta}$ directly into the controller as shown in Fig. 1(a), it is also possible to use build-in signals for diagnosis, Niemann and Poulsen [2008]. In the following, the rotor speed in the wind turbine will be used for this. This will not change the principles in the AFD setup described above; it will only change the injection point for the diagnosis/auxiliary signal.

3.2 Evaluation of residual signals

The injection of a known signal into the system either the auxiliary signal $\boldsymbol{\eta}$ via the control signal $\boldsymbol{u} = \tilde{\mathbf{V}}^{-1}(\tilde{\mathbf{U}}\boldsymbol{y} + \boldsymbol{\eta})$ or if the disturbance signal $\boldsymbol{d}$ is known, can be used to investigate the residual signal $\boldsymbol{\epsilon}$. If e.g. a sinusoidal signal with the frequency ω is injected into the system, the residual will also be a sinusoidal signal with the same frequency. Two new signals can be formed from the residual signal

$$\boldsymbol{c}^\alpha = \boldsymbol{\epsilon}\cos(\omega t + \alpha) \text{ and } \boldsymbol{s}^\alpha = \boldsymbol{\epsilon}\sin(\omega t + \alpha) \tag{17}$$

where α is a specific search direction. A typical choice in connection to wind turbines are 0, 60, 120, 180, 240 and 300 degrees, see the simulation results in section 4.1 and Fig. 2. The signals $\boldsymbol{c}^\alpha$ and $\boldsymbol{s}^\alpha$ can then examined by various detection algorithms. A simple detection algorithm is the CUSUM test, which in a one-sided version is given by

$$z^\alpha_{k+1} = \max\left(z^\alpha_k + \frac{\tau_k}{\sigma}\boldsymbol{c}^\alpha - \frac{\gamma}{2}, 0\right), \tag{18}$$

where τ_k is a time step scaling factor, which for the wind turbine example is $\tau_k = \Omega_{nom}/\Omega$, the scaling factor enables similar detection times for different rotation speeds. The standard deviation of $\boldsymbol{c}^\alpha$ and $\boldsymbol{s}^\alpha$ is denoted σ, and $\boldsymbol{\gamma}$ is a tuning parameter.

3.3 Residual Generator: Extended Kalman Filter

One method to obtain a residual generator is to apply a Kalman filter. Elements from the innovation vector $\boldsymbol{v}$ can then be applied as the residual vector $\boldsymbol{\epsilon}$ given in (15). Due to the fact that the applied wind turbine model is non-linear, an extended Kalman filter (EKF) is used to estimate the states and generate the residuals used by the fault diagnosis algorithm.

The *a posteriori* estimate of the states with the time index $k|k$, meaning estimate at time k given by the knowledge available at time k, is given by

$$\hat{\boldsymbol{x}}^{\boldsymbol{f}}_{k|k} = \hat{\boldsymbol{x}}^{\boldsymbol{f}}_{k|k-1} + \mathbf{L}_k\boldsymbol{v}_k \tag{19}$$

$$\boldsymbol{v}_k = \mathbf{M}_{\mathbf{y},k}(\boldsymbol{y}_k - \boldsymbol{g}(\mathbf{M}^{-1}_{\mathbf{x},k}\hat{\boldsymbol{x}}^{\boldsymbol{f}}_{k|k-1}, \mathbf{M}^{-1}_{\mathbf{u},k}\boldsymbol{u}^{\boldsymbol{f}}_k)) \tag{20}$$

Enabling an *a priori* estimate of the states with the time index $k+1|k$, meaning estimate at time $k+1$ given knowledge available at time k, given by

$$\hat{\boldsymbol{x}}^{\boldsymbol{f}}_{k+1|k} = \underline{\boldsymbol{f}}^{\boldsymbol{f}}(\hat{\boldsymbol{x}}^{\boldsymbol{f}}_{k|k}, \boldsymbol{u}^{\boldsymbol{f}}_k) \tag{21}$$

where the Kalman gain $\mathbf{L}_k$, output error covariance $\boldsymbol{\Psi}_k$ and the discrete time recursive Riccati equation are given by

$$\mathbf{L}_k = \mathbf{P}_{k|k-1}\mathbf{C}^{\mathbf{f}T}_{k|k-1}\boldsymbol{\Psi}^{-1}_k \tag{22}$$

$$\boldsymbol{\Psi}_k = \mathbf{C}^{\mathbf{f}}_{k|k-1}\mathbf{P}_{k|k-1}\mathbf{C}^{\mathbf{f}T}_{k|k-1} + \mathbf{R}_{\mathbf{y}}, \tag{23}$$

$$\mathbf{P}_{k|k} = \mathbf{P}_{k|k-1} - \mathbf{L}_k\mathbf{C}^{\mathbf{f}}_{k|k-1}\mathbf{P}_{k|k-1} \tag{24}$$

$$\mathbf{P}_{k+1|k} = \mathbf{A}^{\mathbf{f}}_{k|k}\mathbf{P}_{k|k}\mathbf{A}^{\mathbf{f}T}_{k|k} + \mathbf{R}_{\mathbf{x}} \tag{25}$$

respectively. The state estimate used by the full-state-feedback control algorithm can either be the *a posteriori* $\hat{\boldsymbol{x}}_{k|k}$ or the *a priori* $\hat{\boldsymbol{x}}_{k|k-1}$.

4. WIND TURBINE EXAMPLE

Active fault diagnosis involves an active probe or excitation signal. However, the wind turbine is already exposed to such a natural excitation signal. As the wind turbine rotates, the blades alternate between high and low wind speeds caused by the spatially distributed turbulent wind field. Also the wind shear, caused by the ground friction,

making the wind speeds nearer ground lower than wind speeds at higher altitudes.

The rotor speed varies more or less with wind speed depending on the mode of operation. At partial load, below rated wind speed, the wind turbine controller attempts to maximize the power capture by keeping the ratio between wind speed and rotor speed at its optimum value. Thus the rotor speed varies and the disturbance signal injected into the system varies in frequency. The rotor azimuth angle ϕ can be used as input to the two residual derived signals

$$\boldsymbol{c} = \boldsymbol{\epsilon}\cos(\phi) \text{ and } \boldsymbol{s} = \boldsymbol{\epsilon}\sin(\phi) \tag{26}$$

or

$$\boldsymbol{c}^{\alpha} = \boldsymbol{\epsilon}\cos(\phi+\alpha) \text{ and } \boldsymbol{s}^{\alpha} = \boldsymbol{\epsilon}\sin(\phi+\alpha) \tag{27}$$

where α is the principal direction (or phase) of investigation.

4.1 Simulation Results

Simulations (100 sec) have been performed with the high fidelity simulation software HAWC2 (Larsen and Hansen [2007]) developed to wind turbine simulations by Risø DTU. The presented simulations are performed with a mean wind speed of 5, 10 and 15 m/s. The wind turbine operates then under both partial and full load conditions. A power law wind shear with coefficient of 0.14 and a Mann turbulence model (Mann [1998]) with turbulence intensity of 0.16 as well as a potential flow tower shadow model is used in the simulation. The wind turbine used in the simulation is the 5 MW reference wind turbine defined in Jonkman et al. [2009].

Four different situations are investigated.

- **0** The nominal case (or the fault free case).
- **1** Offset in in pitch actuator. The offsets are 0.5 deg and 1 deg.
- **2** Offset on edgewise strain gauge sensor. The offsets are 5000 Nm and 10,000 Nm.
- **3** Offset in flapwise strain gauge sensor. The offsets are 500 Nm and 1000 Nm.

The extended Kalman filter presented in Section 3.3 is used as the residual generator. Here, the residuals are the innovations $\boldsymbol{v}_k = \boldsymbol{y}_k - \hat{\boldsymbol{y}}_{\boldsymbol{k}}$ of appropriate sensors (see section 2). In this discussion we are using the edge and flap wise strain gauge sensors (measuring the blade root moment).

The focus of this paper is isolation and the detection problem is thoroughly discussed in Henriksen et al. [2011]. In order to isolate between the faults mentioned above, the mean and variance of c^{α} and s^{α} are determined. The results are presented in Fig. 2 for $\alpha = 0$ i.e. for investigating faults in blade 1. The means and the confidence areas (ellipsoids) are plotted for different faults (and the nominal case). The radii of the ellipsoids encircling the mean values represent standard deviations of the (c^{α}, s^{α})-residuals.

The results are given in Fig. 2. The mean values are indicated with symbols ($\diamond$, $\square$, + and x). The uncertainties are indicated by means of an ellipsoid and a color as given below.

- **0** The nominal case (or the fault free case). Black and $\diamond$.
- **1** Offset in in pitch actuator. Red and $\square$.
- **2** Offset on edgewise strain gauge sensor. Blue and +
- **3** Offset in flapwise strain gauge sensor. Green and x.

If only one sensor is considered (see e.g. panel a in Fig. 2) then an isolation between the different faults is not possible (the sign and the size of fault is unknown). However, if several residuals are combined then an isolation is possible. If for example panels a and d (or b and e or c and f) are combined, then it is easy to isolate faults in flap wise strain gauge sensor from other faults. Other type of faults can be isolated if other sensors are included in the analysis.

5. CONCLUSION

The focus in this paper is fault isolation in wind turbines. This is exemplified by faults in pitch actuator and in sensors for blade root moments (strain gauges). Faults present at only one blade will result in asymmetries, which can easily be detected when using the multi-blade coordinate transformation also known as the Coleman transformation. Active fault diagnosis involves an auxiliary or probing signal. In connection to wind turbine the rotation of the rotor and generator generates an auxiliary signal enabling the monitoring of the turbine. When using the azimuth angle of the rotor as independent variable he proposed method takes the varying rotor speed into account. If combining results from several sensors, a fault can be isolated from others. Single faults in different blades can also be isolated.

REFERENCES

G. Bir. Multi-blade coordinate transformation and its application to wind turbine analysis. In *46th AIAA aerospace sciences meeting and exhibit*, Reno, NV., 2008. [CD ROM].

P. Caselitz and J. Giebhardt. Rotor condition monitoring for improved operational safety of offshore wind energy converters. *Journal of Solor Energy Engineering*, 127 (2):253–261, 2005.

R. P. Coleman and A. M. Feingold. Theory of self-excited mechanical oscillations of helicopter rotors with hinged blades. Technical Report 1351, National Advisory Committee for Aeronautics (NACA), 1958.

P. M. Frank and X. Ding. Frequency domain approach to optimally robust residual generation and evaluation for model-based fault diagnosis. *Automatica*, 30(5):789–804, 1994.

Z. Hameed, Y.S. Hong, Y.M. Cho, S.H. Ahn, and C.K. Song. Condition monitoring and fault detection of wind turbines and related algorithms: A review. *Renewable & sustainable energy reviews*, 13(1):1–39, 2009.

M. H. Hansen. Improved modal dynamics of wind turbines to avoid stall-induced vibrations. *Wind Energy*, 6(2): 179–195, 2003.

L. C. Henriksen and N. K. Poulsen. An online relinearization scheme suited for model predictive or linear quadratic control. IMM-Technical Report 2010-13, Dept. of Informatics and Mathematical Modelling, Technical University of Denmark, 2010.

L. C. Henriksen, H. H. Niemann, and N. K. Poulsen. Detecting asymmetries in the rotor of a wind turbine using the multi-blade coordinate transformation. In

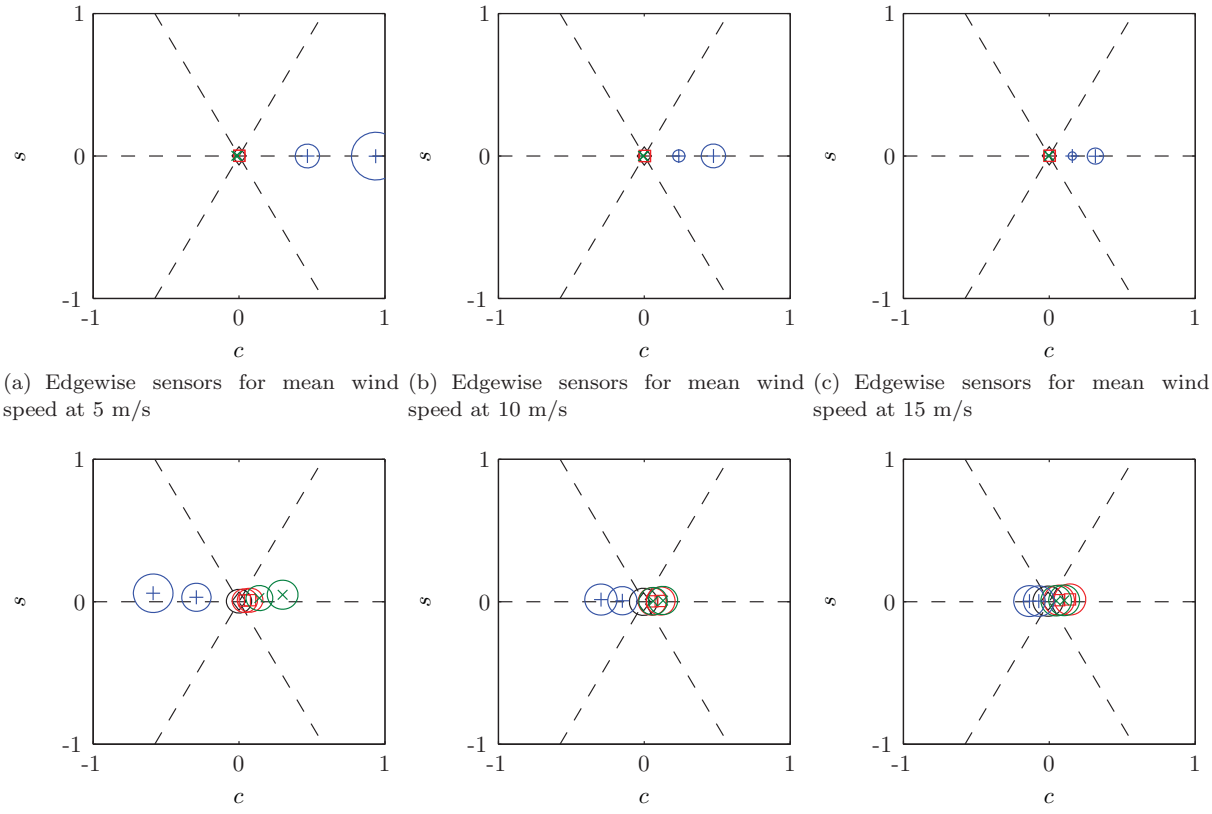

(a) Edgewise sensors for mean wind speed at 5 m/s

(b) Edgewise sensors for mean wind speed at 10 m/s

(c) Edgewise sensors for mean wind speed at 15 m/s

(d) Flapwises sensors for mean wind speed at 5 m/s

(e) Flapwise sensors for mean wind speed at 10 m/s

(f) Flapwise sensors for mean wind speed at 15 m/s

Fig. 2. Mean values of (c, s)-residuals generated by nominal and fault cases for blade root bending sensors in edge- and flapwise directions. The the radii of the ellipsoids encircling the mean values represent standard deviations of the (c, s)-residuals. The fauls are offset in pitch actuator (red and □), offset in strain gauge in flapwise direction (green and x) and strain gauge in edgewise direction (blue and +).

Diagnostics of Processes and Systems, Zamosc, Poland, 2011.

J. Jonkman, S. Butterfield, W. Musial, and G. Scott. Definition of a 5-MW reference wind turbine for offshore system development. Technical Report NREL/TP-500-38060, National Renewable Energy Laboratory, 1617 Cole Boulevard, Golden, Colorado 80401-3393, February 2009.

T. J. Larsen and A. M. Hansen. How 2 HAWC2, the user's manual. Technical Report Risø-R-1597(ver. 3-1)(EN), Risø National Laboratory, 2007.

L. Ljung. *System Identification: Theory for the User*. Prentice Hall, 2nd edition, 1999.

J. Mann. Wind field simulation. *Probabilistic Engineering Mechanics*, 13(4):269–282, 1998.

H. H. Niemann. A setup for active fault diagnosis. *IEEE Transactions On Automatic Control*, 51(9):1572–1578, 2006.

H. H. Niemann and N. K. Poulsen. Information based fault diagnosis. In *Proceedings of the 17th World Congress*, pages 8890–8895, Seoul, South Korea, 2008. International Federation of Automatic Control (IFAC).

P. F Odgaard and J. Stoustrup. Unknown input observer based detection of sensor faults in a wind turbine. In *IEEE International Conference on Control Applications Part of 2010 IEEE Multi-Conference on Systems and Control*, pages 310–315, Yokohama, Japan, 2010.

P. F. Odgaard, J. Stoustrup, R. Nielsen, and C. Damgaard. Observer based detection of sensor faults in wind turbines. In *Online Proceedings of the European Wind Energy Conference*, Marseille, France, 2009. European Wind Energy Association (EWEA).

N. K. Poulsen and H. H. Niemann. Active fault diagnosis - a stochastic approach. In *7th Symposium on Fault Diagnosis, Supervision and Safety of Technical Processes*, pages 603–608, Barcelona, Spain, 2009. International Federation of Automatic Control (IFAC).

T. T. Tay, I. M. Y. Mareels, and J. B. Moore. *High Performance Control*. Birkhäuser Boston, 1st edition, September 1997.

C.-S. Tsai, C.-T. Hsieh, and S.-J. Huang. Enhancement of damage-detection of wind turbine blades via cwt-based approaches. *IEEE Transactions On Energy Conversion*, 21(3):776–781, 2006.

S. J. Watson, B. J. Xiang, W. Yang, P. J. Tavner, and C. J. Crabtree. Condition monitoring of the power output of wind turbine generators using wavelets. *IEEE Transactions On Energy Conversion*, 25(3):715–721, 2010.

X. Wei and M. Verhaegen. Sensor and actuator fault diagnosis for wind turbine systems by using robust observer and filter. *Wind Energy*, 14(4):491–516, 2011.